

Weak-photon-localization effects in nonlinear optical phenomena

V. M. Agranovich and V. E. Kravtsov

Spectroscopy Institute, USSR Academy of Sciences

(Submitted 16 May 1988)

Zh. Eksp. Teor. Fiz. **95**, 484–495 (February 1989)

It is shown that the angular dependence of the intensity of radiation generated in a nonlinear disordered sample should contain characteristic interference peaks due to weak localization of the photons. The shape of the peak reflects the electric-field structure of the radiation that is strongly scattered in the sample, and is sensitive to Anderson localization effects. The angular dependence of second-harmonic generation and of difference-frequency generation in a slab of thickness $L \gg l$ (l is the photon mean free path for elastic scattering) is calculated. Photons of one of the frequencies participating in the nonlinear process are strongly scattered in the slab. The shapes of the interference peaks in various limiting cases are discussed.

1. INTRODUCTION

Light propagation in turbid media has been attracting considerable interest lately. This interest is due principally to the analogies observed when anomalies of the propagation of classical (light or sound) waves in randomly inhomogeneous media are studied and compared with quantum interference effects known to cause Anderson localization in solids.¹

It has been found, however,² that in the case of light it is difficult to meet the Anderson localization condition $\lambda \sim 2\pi l$ (λ is the wavelength and l is the mean free path of elastic scattering of photons by inhomogeneities). Experiments^{3–6} have shown that ordinary inhomogeneous media such as suspensions and pressed powders satisfy the inequality $\lambda \ll 2\pi l$. In this case the interference effects that lead to localization are small, of order $\gamma = \lambda / 2\pi l \ll 1$ (weak localization). It is known nonetheless that the weak localization observed in the optics of turbid media cannot be ignored, in view of the intensity peak produced in backscattering of coherent radiation.⁷ The intensity of this peak at the maximum is equal to the diffuse-background intensity, and its width is a small quantity $\sim \gamma$ (Refs. 3–6, 8–10). Thus, coherent effects in multiple wave scattering lead to qualitative irregularities in a linear optical process such as light reflection. It is natural to expect nonlinear optical effects in randomly inhomogeneous media also to differ qualitatively from processes in transparent media.

We shall discuss here, using three-wave nonlinear processes as an example, those qualitative effects that result from weak localization of photons in a nonlinear disordered medium. In Sec. 2 we consider the angular dependence of second-harmonic generation (SHG) intensity in a nonlinear medium that is transparent to exciting radiation of frequency ω , but scatters the second-harmonic radiation. In Sec. 2 the cross section is calculated, as a function of angle, for difference-frequency generation (DFG) in a medium that scatters one of the incident waves strongly. It will be shown that in both cases the angular dependence of the cross sections for the linear processes should contain peaks similar to the backscattering peak from a disordered medium. We discuss here the shapes of these peaks for various conditions of the nonlinear processes and the connection between these shapes and the character of the photon distribution in a disordered medium.

2. SECOND-HARMONIC GENERATION

We consider SHG in the sample shown in Fig. 1. Let light (frequency ω and wave vector \mathbf{k}_0) impinge on the face of this sample at $z = 0$. We assume that the sample is transparent to this radiation and is optically homogeneous. It is also assumed, however, that the second harmonic radiation is strongly scattered in the sample. This situation can obtain, for example, in doped semiconductors when the frequency 2ω is close to the exciton-resonance frequency ω_0 . In this case,¹¹ elastic scattering of polaritons of frequency 2ω by impurities is enhanced manyfold and predominates over absorption, whereas polaritons of frequency ω are very weakly scattered and are absorbed.

We are interested in the angular distribution of the second harmonic leaving the sample. For simplicity, we consider only the intensity of *s*-polarized radiation of frequency 2ω , for which the electric-field vector is directed along the *y* axis. The energy flux of the *s*-polarized second-harmonic radiation in the direction $\mathbf{n} = (n_x, 0, n_z)$ is determined by the Poynting vector:

$$S(\mathbf{n}) = \frac{ic}{16\pi k} \left(\frac{\partial E^*}{\partial n} E - E^* \frac{\partial E}{\partial n} \right). \quad (1)$$

Here $k = 2\omega/c$, while $E \equiv E_y(2\omega; \mathbf{r})$ is the second-harmonic electric field, which can be expressed in terms of the nonlinear polarization $P^{NL}(\mathbf{r})$ and the wave-equation Green's function $\hat{\mathcal{G}}(\mathbf{r}, \mathbf{r}')$:

$$E_i(\mathbf{r}) = 4\pi k^2 \int d\mathbf{r}' \hat{\mathcal{G}}_{ij}(\mathbf{r}, \mathbf{r}') P_j^{NL}(\mathbf{r}'), \quad (2)$$

where

$$\text{rot rot } \hat{\mathcal{G}} - k^2 \epsilon(\mathbf{r}) \hat{\mathcal{G}} = I \delta(\mathbf{r} - \mathbf{r}'). \quad (3)$$

The nonlinear polarization is defined as

$$P_i^{NL}(\mathbf{r}) = \alpha_{ijl} E_j E_l \exp(2i\mathbf{k}_i \cdot \mathbf{r}), \quad (4)$$

where α_{ijl} is the intrinsic nonlinear polarizability of the medium and is assumed to be known. E_j is the amplitude of the incident electric field of frequency ω and wave vector \mathbf{k}_j inside the sample. The disorder in the system is manifested by the fact that the dielectric constant $\epsilon(\mathbf{r})$ at the frequency 2ω , on which the Green's function $\hat{\mathcal{G}}$ depends, contains within the sample a randomly inhomogeneous component

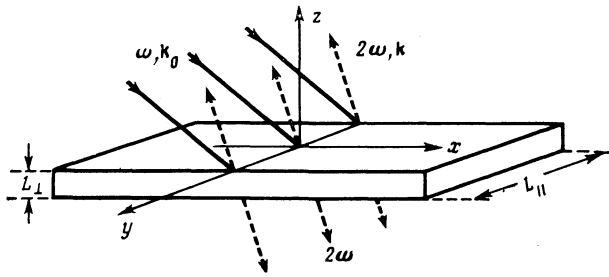


FIG. 1. Geometry of experiment.

$$\varepsilon(\mathbf{r}) = \begin{cases} 1, & z > 0, \\ \varepsilon_1 + \delta\varepsilon(\mathbf{r}), & -L_{\perp} < z < 0 \end{cases}, \quad (5)$$

which we assume for simplicity to be a Gaussian uncorrelated field

$$\langle \delta\varepsilon(\mathbf{r}) \rangle = 0, \quad \langle \delta\varepsilon(\mathbf{r}) \delta\varepsilon(\mathbf{r}') \rangle = \frac{6\pi}{k^4 l} \delta(\mathbf{r} - \mathbf{r}'). \quad (6)$$

Relation (6) is in fact a definition of the mean free path l . The problem of finding the realization-averaged [i.e., averaged over the realizations of the random field $\delta\varepsilon(\mathbf{r})$] energy flux S reduces to substituting (2) in (1) and taking the average $\langle \hat{\mathcal{G}} \hat{\mathcal{G}}^* \rangle$ of the resultant pair of Green's functions. This averaging can be carried out by the usual cross technique¹² based on summation of perturbation-theory series in $\delta\varepsilon(\mathbf{r})$. As a result, the electric-field correlator

$$\langle E_i(\mathbf{r}) E_j^*(\mathbf{r}') \rangle = \langle E_i(\mathbf{r}) \rangle \langle E_j^*(\mathbf{r}') \rangle + K_{ij}(\mathbf{r}, \mathbf{r}'), \quad (7)$$

in terms of which $\langle S \rangle$ is expressed directly, can be represented in the form (see also Ref. 13 and 10)

$$K_{ij}(\mathbf{r}, \mathbf{r}') = \int d\mathbf{r}_1 d\mathbf{r}_2 d\mathbf{r}_3 d\mathbf{r}_4 \langle E_n(\mathbf{r}_1) \rangle \langle E_s^*(\mathbf{r}_2) \rangle \Gamma_{nslm}(\mathbf{r}_1, \mathbf{r}_2, \mathbf{r}_3, \mathbf{r}_4) \times G_{li}(\mathbf{r}_3, \mathbf{r}) G_{mj}^*(\mathbf{r}_4, \mathbf{r}'). \quad (8)$$

Here \hat{G} and $\langle E \rangle$ denote respectively the Fourier components of the averaged Green's functions and of the second-harmonic electric field in the bulk of the sample.

The quantity $\langle E_n \rangle \langle E_s^* \rangle$ plays the role of a source of slow diffusive modes corresponding to an irreducible four-pole diagram Γ . Under weak-localization conditions, the Γ vertex can be represented by an expansion in the parameter γ . The first two terms of this expansion are sums of ladder and fan diagrams and are expressed in terms of the diffusion propagator $D(\mathbf{r}, \mathbf{r}')$ (Refs. 8–10):

$$\Gamma_{mnij}^{(diff)} = l^{-2} \delta(\mathbf{r}_1 - \mathbf{r}_2) \delta(\mathbf{r}_3 - \mathbf{r}_4) \delta_{mn} \delta_{ij} D(\mathbf{r}_1, \mathbf{r}_3), \quad (9)$$

$$\Gamma_{mnij}^{(inter)} = l^{-2} \delta(\mathbf{r}_1 - \mathbf{r}_4) \delta(\mathbf{r}_2 - \mathbf{r}_3) \delta_{mj} \delta_{ni} D(\mathbf{r}_1, \mathbf{r}_2), \quad (10)$$

where $D(\mathbf{r}, \mathbf{r}')$ satisfies the equation¹⁾

$$\frac{l}{3} \nabla^2 D(\mathbf{r}, \mathbf{r}') = -\delta(\mathbf{r} - \mathbf{r}') \quad (11)$$

and the boundary conditions

$$D(\mathbf{r}, \mathbf{r}') + hl \frac{\partial}{\partial n} D(\mathbf{r}, \mathbf{r}') = 0. \quad (12)$$

The dimensionless constant h depends on the conditions of specular reflection of the light from the sample boundaries. The specular reflection of the light is usually weak, and $h \sim 1$

(Ref. 14). For an ideally reflecting boundary, however, $h \rightarrow \infty$, since the normal (to the surface) component of the diffusion flux $J_d \sim \nabla D(\mathbf{r}, \mathbf{r}')$ should vanish in this case. It can be shown that as $R \rightarrow 1$, where R is the angle-averaged specular-reflection coefficient of light impinging on the sample from the outside, the following relation holds:

$$h \sim (1-R)^{-1}. \quad (13)$$

Before proceeding to discuss effects connected with multiply scattered radiation and described by the vertex Γ , we consider the contribution of ballistic photons of frequency 2ω to the angular distribution of the SHG intensity. This contribution is connected with the reducible part $\langle E \rangle \langle E^* \rangle$ of the correlator (7), and to find it we must use (2) to calculate the mean electric field at large distances $r \gg L_{\perp}, L_{\parallel}$ from the sample. The Green's function averaged over the realizations of $\delta\varepsilon(\mathbf{r})$ and needed for these calculations coincides with the Green's function for the case of an ordered system in a sample whose dielectric constant has a small imaginary part $\sim \gamma$ (Ref. 10):

$$\bar{\varepsilon}_1 = \varepsilon_1 + i\varepsilon_1^{1/2}/kl.$$

As a result, we obtain for $\langle E(\mathbf{r}) \rangle$

$$\langle E(\mathbf{r}) \rangle = t_e \alpha_{yjl} E_{1j} E_{1l} \frac{e^{i\mathbf{a}\mathbf{r}}}{4\pi r} I(\mathbf{n}), \quad (14)$$

where t_e is the amplitude coefficient for transmission of radiation of frequency 2ω through the sample boundary (for radiation incident on the sample from the outside). The value of I is determined by the following integral over the sample volume:

$$I(\mathbf{n}) = \int d\mathbf{r}_1 \exp\{i(2\mathbf{k}_1 - \mathbf{k}_2) \cdot \mathbf{r}_1 - (z + L_{\perp})/2l\}, \quad (15)$$

where $l_{*} = lk_{zz}/k_2$; $\mathbf{k}_2(\mathbf{n})$ is the wave vector of the second harmonic in the sample and corresponds, in accordance with the refraction law, to the wave vector $k\mathbf{n}$ in vacuum.

In a transparent sample ($l \rightarrow \infty$) I differs from zero only in a narrow range of frequencies and observation angles, when the phase matching condition, which reflects the photon-momentum conservation law, is met:

$$|(k_2 - 2k_1)_x| \ll 1/L_{\parallel}, \quad (16a)$$

$$|(k_2 - 2k_1)_z| \ll 1/L_{\perp}. \quad (16b)$$

For relatively strong scattering, when $2l_* < L_{\perp}$, a substantial contribution to (15) is made only by a surface layer of thickness $\sim l$. This is a manifestation of the fact that only photons of frequency 2ω generated near the surface (the crosshatched region in Fig. 2) can leave the sample without being scattered at all. As a result, the characteristics of the ballistic peak should be the same in the case $2l_* < L_{\perp}$ as in the transparent sample $2l_*$ thick.

As l decreases, an ever increasing role is assumed by photons multiply reflected in the sample. Their contribution to the SHG intensity is determined essentially by the dynamics of the diffusion modes and is described by the irreducible part of the electric-field correlator (8). To calculate this correlator we find first from (2) and (4) the mean value of the second-harmonic electric field inside the sample:

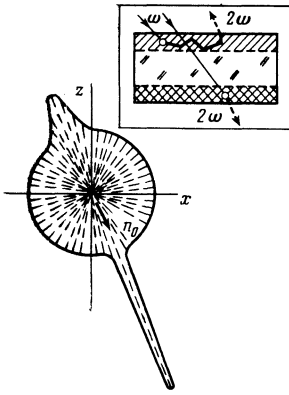


FIG. 2. Qualitative anomalies of the angular distribution of SHG intensity. Here \mathbf{n}_0 is the direction along which the photon-momentum is conserved. The peak in the $-\mathbf{n}_0$ direction is due to interference in multiple scattering of photons of frequency 2ω . The inset shows schematically the SHG in the sample: the isotropic background is due to SHG in the bulk; the peaks are due to SHG in the hatched surface regions.

$$\langle E_i(\mathbf{r}) \rangle = 4\pi A_i \exp(2ik_i \mathbf{r}), \quad (17)$$

where

$$A_i = k^2 G_{ij}(2\mathbf{k}_1) \alpha_{jin} E_{1i} E_{1n}, \quad (18)$$

and $\hat{G}(\mathbf{p})$ is the spatial Fourier component of the volume part of the averaged Green's function:

$$G_{ij}(\mathbf{p}) = \frac{\delta_{ij} - p_i p_j / p^2}{p^2 - k_2^2 - ik_2/l}. \quad (19)$$

Since radiation of frequency ω passes freely through the sample, the amplitude of the averaged second-harmonic electric field is independent of coordinate. This amplitude, however, as seen from (19), is significant only when

$$|2k_1 - k_2| = \Delta(\omega) \ll 1/l. \quad (20)$$

Thus, a second harmonic is effectively generated in a weakly disordered sample ($\gamma \ll 1$) in a narrow range of frequencies satisfying Eq. (20), although this range is significantly broader than for a transparent sample.

For a qualitative understanding of the SHG anomalies that can result from weak photon localization, we note that expression (8) is valid also for linear reflection of light of frequency 2ω from a disordered system. In this case, however,

$$\langle E(\mathbf{r}) \rangle \propto \exp\{i\mathbf{k}_i \mathbf{r} - |z|/2l\}, \quad (21)$$

where \mathbf{k}_i is the wave vector of the incident radiation inside the sample. Comparing (17) with (21) we readily note that they have roughly the same dependence on position if the substitution $2\mathbf{k}_1 \approx \mathbf{k}_i$ is made. Physically this is quite understandable, since the contribution of a multiply scattered photon to the SHG intensity does not depend on whether this photon is the result of a nonlinear process or whether it was incident on the sample from the outside with the same wave vector. In the latter case, however, it is known that the intensity of the reflected light has a peak corresponding to back-scattering: $\mathbf{k}_2 = -\mathbf{k}_1$. Consequently, the angular depen-

dence of the SHG intensity should have a peak at $\mathbf{k}_2 = -2\mathbf{k}_1$, i.e., in a direction opposite to that corresponding to the photon-momentum conservation law (Fig. 2).

A quantitative description of the contribution of multiply scattered photons to the SHG intensity can be obtained by substituting in (8) the expression (17) for the mean electric field, and also the well known expressions for the averaged Green's functions. In this case the vertex Γ^{diff} in (9) corresponds to an isotropic diffusive background in the angular distribution of the SHG intensity [$(d\Phi/d\Omega)$ is the second-harmonic radiation-energy flux in solid-angle units]:

$$\left(\frac{d\Phi}{d\Omega} \right)_{\text{diff}} = |t_e|^2 \frac{c}{8\pi} |A(\omega)|^2 \int \frac{d\mathbf{r} d\mathbf{r}'}{l^2} D(\mathbf{r}, \mathbf{r}') \exp\left(-\frac{|z'|}{l}\right), \quad (22)$$

whereas the vertex $\Gamma^{\text{(inter)}}$ [Eq. (10)] yields an interference peak at $\mathbf{k}_2 = -2\mathbf{k}_1$:

$$\left(\frac{d\Phi}{d\Omega} \right)_{\text{inter}} = |t_e|^2 \frac{c}{8\pi} |A_v(\omega)|^2 \int \frac{d\mathbf{r} d\mathbf{r}'}{l^2} D(\mathbf{r}, \mathbf{r}') \times \exp\left\{i(\mathbf{r}-\mathbf{r}') \cdot (2\mathbf{k}_1 + \mathbf{k}_2) - \frac{|z| + |z'|}{2l}\right\}. \quad (23)$$

Equations (22) and (23) are written here for the stationary case when a monochromatic field of frequency ω is incident on the sample. The factor $\exp(-|z|/2l)$ in (23) shows that the interference peak is due to photons generated in a narrow surface region $\sim 2l$ thick (shown singly hatched in Fig. 2), whereas a contribution to the diffuse background is made by photons generated in the bulk of the sample. For $l \ll L_1$ therefore, the peak is small (proportional to l/L_1) compared with the diffuse background. Note that in pulsed SHG faster than the photon diffusion time through the sample the relative height of the peak can exceed l/L_1 significantly.¹⁵ The shape of the peak is determined by the structure of the diffusion propagator. For a bulky sample with $L_1 \gg d \gg l$, where $d = (l_{\text{in}}/3)^{1/2}$ is the damping length connected with the inelastic processes ($l_{\text{in}} = \text{Im}k_2(\omega)$), the angular dependence of the SHG intensity near the peak can be represented in the form

$$\left(\frac{d\Phi}{d\Omega} \right) = J_0 \left(1 + \beta \frac{f(\theta)}{f(0)} \right). \quad (24)$$

Here $J_0 = \frac{3}{4}(1+h)(1+hl/d)^{-1} |t_e|^2 c |A(\omega)|^2 L_{\parallel}^2 (d/l)$,

$$\beta = \frac{4l}{d} \frac{|A_v|^2}{|A|^2}, \quad (25)$$

and for the case of normal incidence the function $f(\theta)$ which depends on the angle θ between $2\mathbf{k}_1$ and \mathbf{k}_2 ($2|\mathbf{k}_1| \approx |\mathbf{k}_2|$) is

$$f(\theta) = \frac{h + (1+hql)}{(1+hql)(1+2ql)^2}, \quad q^2(\theta) = k_2^2 \theta^2 + d^{-2}. \quad (26)$$

The peak takes an entirely different form for a cavity in the form of thin slab with strong specular reflection from its faces. For $L_1 \ll hl \ll d$ the photon diffusion in such a cavity is quasi-two-dimensional—the propagator $D(r, r')$ does not depend on the transverse coordinates z and z' . In this case the SHG intensity can also be represented in the form (4), but d in (25) must be replaced by the thickness L_1 of the cavity, and the background intensity J_0 is given by

$$J_0 = \frac{3}{8} h |t_e|^2 c |A(\omega)|^2 L_{\parallel}^2 (L_{\perp}/l). \quad (27)$$

In this quasi-two-dimensional system the function $f(\theta)$, and with it the interference peak, takes the Lorentz form

$$f(\theta) = \kappa^2 / (\kappa^2 + q^2(\theta)), \quad (28)$$

where $\kappa^2 = 2(hlL_{\perp})^{-1}$. The quantity $D^2 \kappa \sim c(1-R)/L_{\perp}$ (D is the photon diffusion coefficient) is the reciprocal of the time needed by a photon of frequency 2ω to leave the cavity, and the function $f(q)$ [Eq. (28)] is proportional to the diffusion propagator for such a cavity with strong Rayleigh scattering. Neglecting damping, the width of the interference peak should decrease without limit²⁾ as $R \rightarrow 1$. Its value, however, remains fixed here, since it follows from (13) that $h|t_e|^2 \sim 1$ as $R \rightarrow 1$. On the contrary, the ballistic peak vanishes as $R \rightarrow 1$. The reason why the contribution of multiply scattered photons to the SHG intensity does not decrease as $R \rightarrow 1$ is that under stationary conditions the SHG intensity is determined only by the intensity of the incident light of frequency ω , which is not strongly reflected. It is this possibility of separating the contribution of multiply scattered photons which ensures constancy of the signal as $R \rightarrow 1$ and is a major advantage of the use of nonlinear processes to investigate the kinetic properties of photons in quasi-two-dimensional optical systems, where the Anderson-localization effects are particularly strong.

3. DIFFERENCE-FREQUENCY GENERATION IN A DISORDERED SAMPLE

In contrast to the preceding section, we consider here a situation wherein the medium scatters strongly not only the generated but also the excited radiation. Let two coherent light beams with frequencies ω_1 and ω_1' and wave vectors (in the sample) \mathbf{k}_1 and \mathbf{k}_1' be incident on the sample shown in Fig. 1. Three-wave mixing results in generation of radiation at the difference frequency $\omega_2 = \omega_1 - \omega_1'$. We assume that the sample is transparent to the ω_1' and ω_2 beams, but scatters strongly the ω_1 beam. This situation is possible, e.g., in an impurity semiconductor, when the frequency ω_1 lies near the exciton resonance and the frequencies ω_1' and ω_2 lie deep in the forbidden band.¹¹

The angular distribution of the radiation intensity at the difference frequency ω_2 can be easily expressed in terms of the correlator of the nonlinear polarizabilities:

$$\frac{d\Phi}{d\Omega} = \frac{\omega_2^4}{8\pi c^3} (\delta_{ij} - n_i n_j) \int d\mathbf{r}_1 d\mathbf{r}_2 \langle P_i^{NL}(\mathbf{r}_1) P_j^{NL*}(\mathbf{r}_2) \rangle \times \exp[-i\mathbf{k}_2(\mathbf{r}_1 - \mathbf{r}_2)], \quad (29)$$

where \mathbf{n} is a unit vector in the radiation direction, while $\mathbf{k}_2(\mathbf{n})$ is the wave vector of the ω_2 radiation inside the sample and corresponds, according to the refraction law, to a wave vector $\omega_2 \mathbf{n}/c$ in vacuum. Equation (29) can be obtained directly from the expression for the cross section for Rayleigh scattering of light by the fluctuations $\delta\epsilon$ by replacing the inhomogeneous part $\delta\epsilon E$ of the induction vector by $4\pi \mathbf{P}^{NL}$. In the case considered here,

$$P_i^{NL}(\mathbf{r}) = \alpha_{ijl} E_j(\omega_1; \mathbf{r}) E_l^*(\omega_1'; \mathbf{r}), \quad (30)$$

where $\mathbf{E}(\omega_1; \mathbf{r})$ and $\mathbf{E}(\omega_1'; \mathbf{r})$ are the amplitudes of the radiation electric fields of frequencies ω_1 and ω_1' . Since the sample is assumed to be transparent to the frequency ω_1' , we have $\mathbf{E}(\omega_1'; \mathbf{r}) = \mathbf{E}(\omega_1') \exp(i\mathbf{k}_1' \mathbf{r})$. Equation (29) is reduced as a result to

$$\frac{d\Phi}{d\Omega} = \frac{\omega_2^4}{8\pi c^3} F_{ij}(\mathbf{n}) \int d\mathbf{r}_1 d\mathbf{r}_2 \langle E_i(\omega_1; \mathbf{r}_1) E_j^*(\omega_1; \mathbf{r}_2) \rangle \times \exp[-i(\mathbf{k}_2 + \mathbf{k}_1')(\mathbf{r}_1 - \mathbf{r}_2)], \quad (31)$$

where

$$F_{ij}(\mathbf{n}) = (\delta_{in} - n_i n_n) \alpha_{isa} \alpha_{nmj}^* E_s^*(\omega_1') E_m(\omega_1'). \quad (32)$$

The intensity angular dependence (31) thus contains direct information on the spatial distribution of the electric field of the strongly scattering radiation of frequency ω_1 . Any singularity in the correlation function $\langle EE^* \rangle$ of the electric fields, particularly one connected with Anderson localization of photons having the frequency ω_1 , should be manifested in the character of the angular dependence of the generated radiation with frequency ω_2 . We shall consider below in detail the form of the angular dependence (31) in the weak-localization case $\gamma \ll 1$.

The electric-field correlator of the radiation scattered inside the sample can be obtained from (7) and (8). In this case $\langle \mathbf{E}(\mathbf{r}) \rangle$ is given by¹⁰

$$\langle E_i(\mathbf{r}) \rangle = t_e E_i^{(0)}(\omega_1) \exp[i\mathbf{k}_1 \mathbf{r} - |z|/2l_*], \quad l_* = l|k_{1z}|/k_1, \quad (33)$$

where $\mathbf{E}^{(0)}(\omega_1)$ is the amplitude of the incident electric field of frequency ω_1 and t_e is the amplitude transmission coefficient for this field. Just as in the situation considered in the preceding section, the reducible part of the correlator describes the contribution of the ballistic photons to the DFG intensity:

$$\left(\frac{d\Phi}{d\Omega} \right)_{ball} = \frac{\omega_2^4}{8\pi c^3} F(\mathbf{n}) |t_e|^2 \left| \int d\mathbf{r}_1 \exp \left[i(\mathbf{k}_1 - \mathbf{k}_1' - \mathbf{k}_2) \mathbf{r}_1 - \frac{|z_1|}{2l_*} \right] \right|^2, \quad (34)$$

where

$$F(\mathbf{n}) = (\delta_{ij} - n_i n_j) \alpha_{isa} \alpha_{imn}^* E_s^*(\omega_1') E_m(\omega_1') E_l^{(0)}(\omega_1) E_n^{(0)*}(\omega_1).$$

The DFG angular dependence given by (34) takes the form of a sharp peak in the direction corresponding to the momentum conservation law $\mathbf{k}_2 = \mathbf{k}_1 - \mathbf{k}_1'$ (peak a in Fig. 3).

The diffuse contribution to the DFG is determined by the vertex $\Gamma^{(diff)}$ [Eq. (9)] in the correlator (8). Substituting (33) and (9) in (8) and using (14) (with replacement $\mathbf{k}_2 \rightarrow \mathbf{k}_1$ for the bulk part of the Green's function $G(\mathbf{p})$, we get

$$\begin{aligned} & \langle E_i(\omega_1; \mathbf{r}) E_j^*(\omega_1; \mathbf{r}') \rangle_{diff} \\ &= N(h, z) |t_e|^2 |E^{(0)}(\omega_1)|^2 (k_{1z}/k_1) \left(\delta_{ij} + \frac{1}{k_1^2} \frac{\partial^2}{\partial r_i \partial r_j} \right) \\ & \times \left\{ \frac{\sin k_1 |\mathbf{r} - \mathbf{r}'|}{k_1 |\mathbf{r} - \mathbf{r}'|} \exp \left[-\frac{|\mathbf{r} - \mathbf{r}'|}{2l} \right] \right\}, \end{aligned} \quad (35)$$

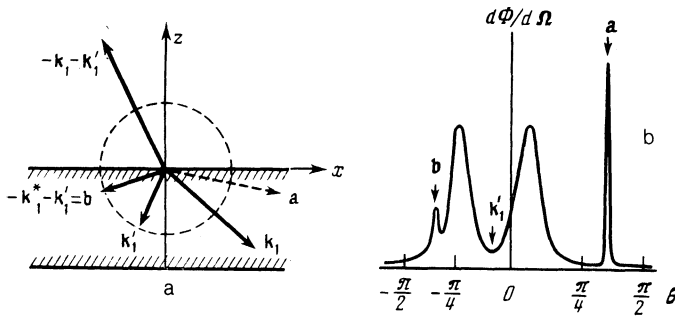


FIG. 3. a) Geometry of DFG. The radius of the dashed circle is equal to k_2 . b) Angular dependence of the DFG intensity: the peak in the **a** direction corresponds to the photon-momentum conservation law; the peak in the **b** direction superposed on the broader diffuse peak is due to weak localization of the photons of frequency ω_1 .

where $N(h, z) = \frac{3}{4}(1+h)(h+L_1/2l)^{-1}(h+(L_1-z)/l)$.

The correlator (35) is isotropic. Nonetheless, it makes a strongly anisotropic contribution to the angular distribution of the DFG, owing to the presence of a preferred direction—that of the wave vector \mathbf{k}'_1 of the radiation with frequency ω'_1 :

$$\left(\frac{d\Phi}{d\Omega}\right)_{diff} = \frac{J_1(\mathbf{n})}{1+(l^2/k_1^2)[(\mathbf{k}'_1+\mathbf{k}_2)^2-k_1^2]^2} \frac{L_\perp}{l}, \quad (36)$$

where we have as $l_{in} \rightarrow \infty$

$$J_1 = \frac{3}{8} F_{im}(\mathbf{n}) (\delta_{im} - n_i n_m) (1+h) |t_e|^2 |E^{(0)}(\omega_1)|^2 \frac{\omega_2^4 k_{1z} l^2}{k_1^3 c^3} L_\parallel^2.$$

With this choice of frequencies, when

$$k_1' + k_2 > k_1 > |k_1' - k_2|, \quad (37)$$

the DFG angular distribution should have two peaks of width $\sim \lambda/l$ (Fig. 3). It is easily seen from (36) that the integrated intensity of these peaks does not depend on l (for $l \ll L_1$), and their height, according to (13), does not decrease as $t_e \rightarrow 0$.

The above contributions (34) and (36) to the DFG intensity contain no information on the structure of the diffusion propagator $D(\mathbf{r}, \mathbf{r}')$ and are thus insensitive to Anderson-localization manifestations. This information is contained only in that part of the correlator $\langle EE^* \rangle$ which is due to interference in the case of multiple scattering, and is determined in the lowest order in γ by the vertex $\Gamma^{(inter)}$ (10). This part of the correlator is determined by scattered-photon trajectories located near the sample surface ($|z| \lesssim l$), and to calculate it we must use in (8) the Green's functions $G_{ij}(\mathbf{r}, \mathbf{r}')$ that take into account surface terms:

$$G_{ij}(\mathbf{r}, \mathbf{r}') = (\delta_{ij} + k_1^{-2} \nabla_i \nabla_j) G(\mathbf{r}, \mathbf{r}'), \quad (38)$$

where the scalar Green's function is

$$G(\mathbf{r}, \mathbf{r}') = \int G(\mathbf{q}, z, z') e^{i\mathbf{q} \cdot (\boldsymbol{\rho} - \boldsymbol{\rho}')} \frac{d^2 \boldsymbol{\rho}}{(2\pi)^2} \quad (39)$$

with

$$G(\mathbf{q}, z, z') = \frac{1}{2ik_{1q}} \{e^{ik_{1q}|z-z'|+r_i} e^{-ik_{1q}(z+z')}\}. \quad (40)$$

In (39), $\mathbf{r} = (\boldsymbol{\rho}, z)$, r_i is the amplitude coefficient of specular reflection of radiation of frequency ω_1 from an inner surface of the sample, and

$$k_{1q}^2 = k_1^2 - q^2 + ik_1 l. \quad (41)$$

The second term in the curly brackets of (40) is exponentially small for $|z| \gg l$ and $|z'| \gg l$, and describes the surface contribution to $G(\mathbf{r}, \mathbf{r}')$. To avoid misunderstandings, we emphasize that expressions (38)–(41) define the Green's function for a system with a single interface, and the disordered medium occupies the half-space $z < 0$. In the cases $L_1 \gg l$ we are considering, the contribution to $G(\mathbf{r}, \mathbf{r}')$ from the second interface is exponentially small, $\propto \exp(-L_1/l)$, and is not taken into account.

As a result, using (31)–(41), (33), and (10), we get from (8) ($|\boldsymbol{\rho} - \boldsymbol{\rho}'| \gg l$)

$$\begin{aligned} \langle E_i(\omega_1; \mathbf{r}) E_j^*(\omega_1; \mathbf{r}') \rangle_{inter} &= |t_e|^2 E_i^{(0)}(\omega_1) E_j^{(0)*}(\omega_1) e^{-ik_{1x}(x-x')} \\ &\times \int \frac{dz_1 dz_2}{l^2} e^{ik_{1z}(z_1-z_2)} D(\boldsymbol{\rho} - \boldsymbol{\rho}', z_1, z_2) G(k_{1x}, z_2, z) \\ &\times G^*(k_{1x}, z_1, z') \exp\left[-\frac{|z_1| + |z_2|}{2l}\right]. \end{aligned} \quad (42)$$

For simplicity it was assumed in the derivation of (42) that the incident light of frequency ω_1 is *s*-polarized: $\mathbf{E}^{(0)}(\omega_1) = (0; E^{(0)}(\omega_1); 0)$, $\mathbf{k}_1 = (k_{1x}; 0; k_{1z})$. Expression (42) is substantially simpler for a quasi-two-dimensional system with $hl \gg L_1$, when the diffusion propagator $D(\boldsymbol{\rho} - \boldsymbol{\rho}', z_1, z_2)$ is independent of z :

$$\begin{aligned} \langle E_i(\omega_1; \mathbf{r}) E_j(\omega_1; \mathbf{r}') \rangle_{inter} &= \frac{3\pi}{2k_1^2} |t_e|^2 E_i^{(0)}(\omega_1) E_j^{(0)*}(\omega_1) D(\boldsymbol{\rho} - \boldsymbol{\rho}') \\ &\times e^{-ik_{1x}(x-x')} (e^{-ik_{1z}(z-z')} + |r_i|^2 e^{ik_{1z}(z-z')}) \exp\left[-\frac{|z| + |z'|}{2l}\right], \end{aligned} \quad (43)$$

where

$$D(\boldsymbol{\rho}) = \int e^{i\mathbf{q} \cdot \boldsymbol{\rho}} d(\mathbf{q}) \frac{d\mathbf{q}}{(2\pi)^2}, \quad d(\mathbf{q}) = (lL_\perp)^{-1} (q^2 + \kappa^2)^{-1}. \quad (44)$$

In the opposite limiting case of a thick sample, $L_1 \gg hl$, Eq. (42) also reduces to (43), but then

$$d(\mathbf{q}) = \frac{h + (1+qlh)k_{1z}/2k_1}{(1+qlk_{1z}/k_1)^2 (1+qlh)} \quad (45)$$

Just as the ballistic contribution $\langle E \rangle \langle E^* \rangle$, the interference contribution (42) to the correlator $\langle EE^* \rangle$ differs from zero only in the surface region $|z|, |z'| \lesssim l$. This is precisely why it depends substantially on the specular-reflection coef-

ficient $R_i = |r_i|^2$ of light of frequency ω_1 from the inner surface of the sample. The main distinctive feature of (42) is that it contains terms proportional to

$$\exp[-ik_1(\mathbf{r}-\mathbf{r}')] \text{ and } \exp[-ik_1^*(\mathbf{r}-\mathbf{r}')], \quad (46)$$

where $\mathbf{k}_1^* = (k_{1x}; 0; -k_{1z})$. The presence of the contributions (46) means that in a narrow surface layer of thickness $\sim l$ the average energy flux of radiation of frequency ω_1 contains, besides the ballistic part in the \mathbf{k}_1 direction, additional energy fluxes in the direction of the vectors $-\mathbf{k}_1$ and \mathbf{k}_1^* . On the whole, the structure of the interference part (43) of the correlator $\langle EE^* \rangle$ is similar to the structure of the ballistic part subject to the substitution

$$\mathbf{k}_1 \rightarrow -\mathbf{k}_1 \quad \text{or} \quad \mathbf{k}_1 \rightarrow -\mathbf{k}_1^*. \quad (47)$$

As already noted, the ballistic part of the correlator leads to a peak in the DFG angular dependence, in a direction corresponding to the momentum-conservation law:

$$\mathbf{k}_2 \approx \mathbf{k}_1 - \mathbf{k}_1'. \quad (48)$$

The interference part of (43) should similarly lead to peaks at

$$\mathbf{k}_2 \approx -\mathbf{k}_1 - \mathbf{k}_1', \quad (49a)$$

$$\mathbf{k}_2 \approx -\mathbf{k}_1^* - \mathbf{k}_1'. \quad (49b)$$

It must be noted, however, that for $l \ll L_1, L_{\parallel}$, where L_{\parallel} is the dimension of the illuminated part of the plate, the momentum uncertainties $\Delta \mathbf{k}$ in the longitudinal and transverse directions can differ greatly. In particular, condition (48) should be accurate to within $(\Delta k)_{\parallel} \sim L_{\parallel}^{-1}$ in the longitudinal direction and $(\Delta k)_{\perp} \sim l^{-1}$ in the transverse one. The relation $(\Delta k)_{\parallel} \ll (\Delta k)_{\perp}$ is valid also for Eq. (49) for sufficiently large $h \gg L_1/l$. In these cases, strictly speaking, the positions of the peaks are determined by the components of (48) and (19) along the longitudinal direction x . Here both equations in (49) yield an identical condition for the interference peak:

$$k_{2x} = -k_{1x} - k_{1x}'. \quad (50)$$

Note that the condition for the appearance of an interference peak (50) and the similar condition $k_{2x} = -2k_{1x}$ for SHG can be obtained from the photon-momentum conservation law in the corresponding nonlinear process, by reversing in this law the sign of the wave vector of the strongly scattered radiation. This qualitative conclusion is valid for any nonlinear process in a turbid medium. It can be applied, in particular, also to nonlinear four-wave mixing processes¹⁷ which are not considered in the present article.

Thus, the positions of the interference peak correlate well with the positions of the ballistic peak and are determined only by the incident-light direction and by the dispersion law. The shapes of the ballistic and interference peaks, however, depend on entirely different factors. The ballistic-peak shape is determined by the spatial coherence of the incident light and by the dependence of its intensity on the coordinates x and y . The shape of the interference peak, on the other hand, contains information on the character of the diffusion of photons of frequency ω_1 and is determined by the value of $d(\mathbf{q})$:

$$\left(\frac{d\Phi}{d\Omega} \right)_{inter} = J_2(\mathbf{n}) d(\mathbf{q}) \left[\frac{1}{1+\delta_+^2} + \frac{R_i}{1+\delta_-^2} \right], \quad (51)$$

where

$$\delta_{\pm} = 2l \cdot (\mathbf{k}_2 + \mathbf{k}_1' \pm \mathbf{k}_1)_z; \quad q^2 = (\mathbf{k}_2 + \mathbf{k}_1' + \mathbf{k}_1)_x^2 + d^{-2},$$

$$J_2(\mathbf{n}) = \frac{F_{yy}}{8\pi} |t_e|^2 |E^{(0)}(\omega_1)|^2 \frac{\omega_2^4 (lk_{1z})^2}{k_1^4 c^3} L_{\parallel}^2, \quad (52)$$

L_{\parallel}^2 is the area of the illuminated part of the sample in the $z = 0$ plane. It is easy to verify that if (49) is exactly satisfied the maximum of the interference peak coincides in position with that of the diffusion peak. The DFG intensity as a function of angle is shown for a small deviation from the exact equations (49) in Fig. 3.

4. CONCLUSION

We note first that we have discussed above only the simplest manifestations of localization effects in nonlinear optical processes. In particular, we have considered only nonlinear processes in which three photons participate. Yet four-wave processes, which are so widely used in solid-state spectroscopy, are also undoubtedly of interest. In addition, we have calculated only mean values, leaving aside the important question of speckles, the aperiodic oscillations of the intensities as functions of observation angle, which are typical of the sample in question.

An important feature of the analysis above was also the fact that we have taken into account the optical nonlinearity only in first-order perturbation theory, and that it served essentially as a tool for the study of the structure of a random radiation electric field in a strongly scattering medium. The interaction between photons of like frequency was disregarded in this approximation. Clearly, however, this interaction sets in even in the Kerr-nonlinearity approximation and its analysis under strong-scattering conditions would undoubtedly be of great interest.

In the present stage, however, it is important to carry experiments out on the simplest situations and to study the possibilities of obtaining, with the aid of nonlinear optical processes, fundamental information on the structure of the electric field in a strongly scattering medium.

The authors thank I. V. Lerner and V. I. Yusdon for numerous helpful discussions.

¹When account is taken of inelastic processes characterized by a damping length l_m it is necessary to make in (11) the substitution $\nabla^2 \rightarrow \nabla^2 - d^{-2}$, where $d = (l_m/3)^{1/2}$.

²If the parameters l/L_1 and γ are not too small, the situation considered in Ref. 16 is possible, in which $\kappa^{-1} \gg r_0$ and $d \gg r_0$, where r_0 is the photon localization radius. In this case the peak width remains finite at $\sim \lambda/r_0$ as $R \rightarrow 1$.

¹E. Abrahms, P. W. Anderson, D. C. Licciardello, and T. V. Ramakrishnan, Phys. Rev. Lett. **42**, 673 (1979).

²S. John, Phys. Rev. Lett. **53**, 2169 (1984). P. W. Anderson, Phil. Mag. **B52**, 505 (1985).

³H. P. Van Albada and A. Lagendijk, Phys. Rev. Lett. **55**, 2692 (1985).

⁴J. Fajans, J. S. Wurtele, G. Bekefi, P. S. Knowles, and K. Xu, *ibid.* **57**, 575 (1986).

⁵M. Kaveh, M. Rosenbluh, I. Erdei, and I. Freund, *ibid.* **57**, 2049 (1986). S. Etamad, R. Thompson, and P. Andrejco, *ibid.* **59**, 1420 (1987).

⁶P. E. Wolf and G. Maret, *ibid.* **55**, 2696 (1985).

⁷V. I. Tatarskii, in: "The Effect of Turbulent Atmosphere on Wave Propagation," National Technical Information Service. Washington, D.C., 1971.

⁸E. Akkermans, P. E. Wolf, and R. Maynard, Phys. Rev. Lett. **56**, 1471 (1986).

- ⁹A. A. Golubentsev, Zh. Eksp. Teor. Fiz. **86**, 47 (1984) [Sov. Phys. JETP **57**, 26 (1984)].
- ¹⁰E. Akkermans, P. E. Wolf, R. Maynard, and G. Maret, J. Phys. (France) **49**, 77 (1988).
- ¹¹V. M. Agranovich, V. E. Kravtsov, and I. V. Lerner, Phys. Lett. **A125**, 435 (1987).
- ¹²A. A. Abrikosov, L. P. Gor'kov, and I. E. Dzhaloshinskii, *Quantum Field-Theoretical Methods in Statistical Physics*, Pergamon, 1965.
- ¹³L. Tsang and A. Ishimaru, J. Opt. Soc. Am. **A2**, 1331 (1985).
- ¹⁴A. Ishimaru, *Wave Propagation and Scattering in Random Media, Vol. I*, Academic, 1978 (Russ. transl., Mir, 1981, p. 149).
- ¹⁵V. M. Agranovich and V. E. Kravtsov, Phys. Lett. **A131**, 378, 387.
- ¹⁶R. Merkovits and M. Kaveh, J. Phys. **C20**, 181 (1987).
- ¹⁷B. Dick, R. M. Hochstrasser, and H. P. Trommsdorff, in: *Nonlinear Optical Properties of Organic Molecules and Crystals, Vol. 1*, ATT Bell Labs., 1987, p. 159.

Translated by J. G. Adashko